

Inhibition of platelet-surface-bound proteins during coagulation under flow I: TFPI

Kenji Miyazawa,¹ Aaron L. Fogelson,^{2,3} and Karin Leiderman^{4,5,*}

¹Quantitative Biosciences and Engineering, Colorado School of Mines, Golden, Colorado; ²Department of Mathematics, University of Utah, Salt Lake City, Utah; ³Department of Biomedical Engineering, University of Utah, Salt Lake City, Utah; ⁴Mathematics Department, University of North Carolina at Chapel Hill, Chapel Hill, North Carolina; and ⁵Computational Medicine Program, University of North Carolina at Chapel Hill, Chapel Hill, North Carolina

ABSTRACT Blood coagulation is a self-repair process regulated by activated platelet surfaces, clotting factors, and inhibitors. Tissue factor pathway inhibitor (TFPI) is one such inhibitor, well known for its inhibitory action on the active enzyme complex comprising tissue factor (TF) and activated clotting factor VII. This complex forms when TF embedded in the blood vessel wall is exposed by injury and initiates coagulation. A different role for TFPI, independent of TF:VIIa, has recently been discovered whereby TFPI binds a partially cleaved form of clotting factor V (FV-h) and impedes thrombin generation on activated platelet surfaces. We hypothesized that this TF-independent inhibitory mechanism on platelet surfaces would be a more effective platform for TFPI than the TF-dependent one. We examined the effects of this mechanism on thrombin generation by including the relevant biochemical reactions into our previously validated mathematical model. Additionally, we included the ability of TFPI to bind directly to and inhibit platelet-bound FXa. The new model was sensitive to TFPI levels and, under some conditions, TFPI could completely shut down thrombin generation. This sensitivity was due entirely to the surface-mediated inhibitory reactions. The addition of the new TFPI reactions increased the threshold level of TF needed to elicit a strong thrombin response under flow, but the concentration of thrombin achieved, if there was a response, was unchanged. Interestingly, we found that direct binding of TFPI to platelet-bound FXa had a greater anticoagulant effect than did TFPI binding to FV-h alone, but that the greatest effects occurred if both reactions were at play. The model includes activated platelets' release of FV species, and we explored the impact of varying the FV/FV-h composition of the releasate. We found that reducing the zymogen FV fraction of this pool, and thus increasing the fraction that is FV-h, led to acceleration of thrombin generation.

SIGNIFICANCE We developed a novel mathematical model of flow-mediated coagulation that was sensitive to changes in TFPI levels, especially at low tissue factor densities, which is consistent with experimentally observed effects of TFPI under flow. The sensitivity of the system was entirely due to inhibition reactions that occurred on activated platelet surfaces. TFPI is a potential therapeutic target to rescue thrombin generation in bleeding disorders; thus, our model, which is based on recent discoveries about its inhibitory mechanism, could serve as powerful tool to explore the role of TFPI as a modifier of thrombin generation.

INTRODUCTION

Hemostasis is a self-defense mechanism initiated by a vascular injury, whereby a blood clot forms to stop bleeding. It consists of two intertwined processes, platelet aggregation and coagulation, that begin when the injury exposes subendothelial collagen and tissue factor (TF), respectively. Platelets adhere to the collagen and become

activated, which enhances their ability to aggregate and plug the injury. They also expose phospholipid binding sites on their surfaces to which plasma proteins, called clotting factors, can bind. Activated platelets release proteins from internal stores, including additional clotting factors, inhibitors, and agonists that further platelet activation (1,2). Coagulation is a network of enzymatic reactions that involves clotting factors and inhibitors and culminates in the production of the enzyme thrombin. Thrombin cleaves the soluble plasma protein fibrinogen to form insoluble fibrin, which polymerizes to form a cross-linked hydrogel that physically stabilizes the growing platelet aggregates.

Submitted January 8, 2022, and accepted for publication November 15, 2022.

*Correspondence: karin.leiderman@unc.edu

Editor: Mark Alber.

<https://doi.org/10.1016/j.bpj.2022.11.023>

© 2022 Biophysical Society.

This is an open access article under the CC BY-NC-ND license (<http://creativecommons.org/licenses/by-nc-nd/4.0/>).



Thrombin generation is necessary to the clotting process and is accomplished by the sequential formation of three enzyme-cofactor complexes. One is formed on the injured vascular wall by TF (cofactor) and activated coagulation factor VIIa (FVIIa), and the other two are formed on the surfaces of activated platelets by coagulation factors VIIIa (cofactor) and IXa (the FVIIIa:FIXa “tenase” complex) and by coagulation factors Va (cofactor) and Xa (the FVa:FXa “prothrombinase” complex). It is the prothrombinase complex that enzymatically converts the plasma protein prothrombin into thrombin. Because of the essential roles of the platelet-bound enzyme complexes, the availability of binding sites on the surfaces of activated platelets for the coagulation factors that form these complexes is an important regulator of coagulation; robust thrombin generation does not occur if these complexes cannot form. Furthermore, the requirement that important coagulation reactions occur on activated platelets helps localize coagulation to the site of injury instead of it being spread throughout the vasculature by the flowing blood. The coagulation process involves positive and negative feedback loops, which enable thrombin generation to exhibit threshold-like behavior; substantial thrombin generation occurs only after a sufficient level of TF is exposed. On the other hand, a lack of sufficient inhibitors, which take part in the negative feedback loops, may lead to excessive clot growth and thrombosis, while abnormally high concentrations of inhibitors may impede coagulation and lead to excessive bleeding. The many regulators of clotting normally work together to maintain a proper balance between promoting and inhibiting processes. Bleeding and clotting disorders that manifest as deficiencies or mutations in clotting proteins, such as hemophilia, can disrupt this balance, with serious consequences.

Tissue factor pathway inhibitor (TFPI) has long been regarded as a key inhibitory regulator of coagulation. It is best known for its inhibition of TF:VIIa activity owing to formation of a quaternary complex that includes TF:VIIa, TFPI, and FXa, but more recently has become known to inhibit through FV (more details of this are given below). In humans, there are two TFPI types: TFPI α and TFPI β (3,4). In this study, we focus only on TFPI α . TFPI α is found in human plasma (4) and is also released from platelets upon the platelets’ activation (5). TFPI α contains three Kunitz domains and a C-terminus tail. TFPI binds to TF:VIIa and FXa through its Kunitz 1 and 2 domains, respectively (6,7), and to protein S via Kunitz 3 domain (3). It binds to some FV variants through the C-terminus tail, which is important for its inhibitory action.

Coagulation factor V (FV) is another essential protein for thrombin generation. In its fully cleaved/activated form (FVa), it serves as the cofactor for FXa within the prothrombinase complex that converts prothrombin to thrombin (8,9). In 2001, a novel bleeding disorder was discovered in a family from East Texas (10) that was

related to FV (11). A genetic mutation caused increased expression of an alternative form of FV that was “partially” cleaved and thus named FV-short. Later, FV-short was shown to bind tightly to TFPI α , which was in line with the observed increased levels of TFPI α in the East Texas family. It is now believed that the increased TFPI α levels are the cause of their bleeding phenotype (12). Since the FV-short discovery, it has been recognized that normal FV is physiologically cleaved into two different forms through distinct mechanisms: FXa cleaves what is called the basic region of the B domain, leading to what we call the partially cleaved/activated form (13,14), and thrombin cleaves the entire B domain, leading to the fully cleaved/activated form (15). There is some evidence that FXa can fully cleave FV into FVa, but it does so rather inefficiently (16,17).

Variants of FV are stored in a platelet’s α -granules and secreted after the platelet is activated. (8,18,19). Platelet-secreted FV may be partially or fully cleaved, but there are little data in the literature on the detailed make-up of platelet-secreted FV molecules or on their susceptibility to be bound by TFPI α . In the rest of this paper, we denote the partially cleaved or platelet stored FV as FV-h, for half-cleaved/activated, and FVa as the fully activated form. Of note, FV-short, FV-h, and FVa possess similar cofactor activity within the prothrombinase complex, but only FV-short or FV-h can bind to TFPI α (20).

Early biochemical studies showed that TFPI α has varying effects on thrombin generation depending on the forms of FV that are present. Mast and Broze (21) performed prothrombin activation assays with mixtures containing prothrombin, FXa, lipids, TFPI α , and varying forms of FV. With FVa and FXa, addition of TFPI α produced modest inhibition of thrombin generation. With FV and FXa, however, addition of TFPI α substantially impeded thrombin generation. Interestingly, when FV was preincubated with FXa, subsequent addition of TFPI α had a decreased inhibitory effect (i.e., more thrombin was generated) in comparison with the case in which FV, FXa, and TFPI α were added at the same time. These results suggest that TFPI α inhibits thrombin generation through a variety of mechanisms that could act before and/or after the formation of prothrombinase (with either FV-h or FVa). The presence of lipids may also have enhanced or mediated the inhibitory mechanisms in that study. In later biochemical studies, TFPI α was shown to inhibit prothrombinase early in thrombin generation via FV-h (13,22). It was suggested that TFPI α inhibits thrombin generation through multiple mechanisms, including direct binding of TFPI α with FV-h, interactions with FV-h in ways that either prevent FXa from binding FV-h or that cause it to bind in a way that does not promote thrombin generation, and of course the well-known binding interaction between TFPI α and FXa (22). The relative importance of these various mechanisms and

interactions, along with the effects of lipid or platelet surfaces on them, remains unclear.

Mathematical models are powerful tools that can be used to gain insight into complex biological systems. Our group has developed mechanistic, experimentally validated mathematical models of flow-mediated coagulation that have led to novel insights related to phenotypic variation observed in bleeding and thrombotic disorders (23–28). These models include activated platelet surfaces as the site of many coagulation reactions, thus allowing the availability of these surfaces and their properties to regulate coagulation. In simulations with our previous models, procoagulant platelet-surface reactions are critical to the production of thrombin. The availability of binding sites on the procoagulant surfaces of platelets deposited onto the injury play an important regulatory role. Other mathematical models that simulate thrombin generation in the absence of flow (29) have also shown that thrombin generation is sensitive to variation in normal levels of clotting factors in healthy individuals (30) and in hemophilia (31); these models generally assume that the reactions occur in the presence of an excess of lipid surfaces and do not look specifically at events on limited platelet surfaces as regulators of coagulation.

Collectively, these experimental and mathematical findings raise the question: would blocking the binding of TFPI α to FXa and/or FV-h on the platelet surface rescue thrombin generation in hemophilia? Platelet-surface-dependent, TFPI α -mediated inhibition has not yet been included in any mathematical models of coagulation. We extended our previous model of flow-mediated coagulation to include a detailed description of platelet-surface-mediated TFPI α inhibition, via platelet-bound FXa and FV-h. In our previous model, TFPI α was assumed to bind FXa in the plasma phase and the TFPI α :Xa complex could subsequently bind to TF:VIIa. However, TFPI α had very little impact on thrombin generation through this mechanism because the overwhelmingly dominant inhibitor was dilution of fluid-phase enzymes and active cofactors as flow carried them downstream away from the injury. This was true for all shear rates examined with the model (23). An alternative mechanism of TFPI α inhibition of TF:VIIa, in which TFPI α binds to TF:VIIa:Xa, was also investigated in this model, and it was found that for this mechanism to work, FXa would have to remain bound to TF:VIIa for a long time, in which case its own presence could inhibit TF:VIIa without a role for TFPI α (24).

A major motivation for the current study is to explore the effectiveness of platelet-surface anticoagulant reactions in the regulation of thrombin generation under flow. To our knowledge, our studies are the first to examine the effect of TFPI- and antithrombin (AT)-mediated inhibition occurring directly on platelet surfaces with modeling (we studied AT inhibition with and without heparin in a companion study (32)). The key new additions to the model in this paper are that 1) FV can be partially activated to FV-h by FXa, 2)

FV-h can bind FXa to form active prothrombinase on the platelet surface, 3) TFPI α can directly bind to FV-h in the fluid or bound to the platelet surface, and 4) TFPI α can bind directly to FXa that is bound to the platelet surface. The aforementioned experiments suggested that early in the coagulation reactions, before much thrombin has been generated, active prothrombinase forms on activated platelet surfaces by binding of FXa and FV-h, and that the activity of FXa, FV-h, and/or the prothrombinase formed from them is significantly impacted by TFPI α .

The assumptions regarding TFPI α resulted in many binding combinations that either interfered with the formation of prothrombinase or directly inhibited the already formed complex. We studied how the additional TFPI α inhibition affected the TF threshold for various shear rates and whether inhibition via FXa or FV-h had a larger inhibitory effect. Our results demonstrated new and significant sensitivity of simulated thrombin generation to TFPI α levels that was entirely due to inhibition reactions occurring on platelet surfaces. Direct binding of TFPI α to FXa on the platelet surface had a somewhat stronger inhibitory effect than binding to FV-h when each was considered in isolation, but the greatest inhibitory effect occurred when both mechanisms were at play.

MATERIALS AND METHODS

Previous mathematical model review

Here we give a brief review of our previously developed mathematical model of flow-mediated coagulation (23–25). More details about this model and its sensitivity to parameters can be found elsewhere (27). The model simulates the coagulation reactions occurring in a small reaction zone (RZ) above an injury where TF in the subendothelium (SE) is exposed (Fig. S1). Clotting factors and platelets are transported into and out of the RZ by a combination of flow and diffusion, using a mass transfer coefficient whose value is a function of vessel and injury size, the flow's shear rate, and the species' diffusivity. Clotting factor concentrations in the RZ change owing to their involvement in the coagulation reactions, their binding with activated platelets, and transport in and out of the zone. Similarly, platelet concentrations change as platelets adhere to the injured wall and become activated, and as other platelets are transported in and out of the zone. As platelets build up in the RZ, the height and volume of the RZ increase with the volume of plasma and concentration of platelets in it changing accordingly. Deposition of platelets also blocks the activity of TF:VIIa on the subendothelium in proportion to the fraction of the subendothelium which the platelets cover. The concentration of each species in the RZ plasma is tracked with an ordinary differential equation; this choice relies on the assumption that each species is uniformly distributed (well-mixed) within the reaction zone. An additional well-mixed endothelial zone (EZ) is located adjacent to the RZ, in the direction perpendicular to the flow, with height equal to that of the RZ and width dependent on the flow shear rate and protein diffusion coefficients. The EZ is where active protein C (APC) is produced by a complex formed by thrombomodulin in that zone and thrombin that has diffused to the EZ from the RZ. This APC either diffuses into the RZ or is carried away by the flow.

There are three forms of platelets in the model: unactivated platelets that exist in the plasma phase, activated platelets that are directly attached to SE, and activated platelets in the thrombus that are not directly attached

to SE. Activation of platelets is achieved by contact with the SE, interaction with thrombin, or by exposure to already activated platelets (this is an indirect way to model release of agonists from platelet stores). Activated platelets provide the membrane surface necessary for coagulation factors to bind and react. Each activated platelet expresses specified types and numbers of binding sites to which coagulation proteins can selectively bind.

New model extensions

The key new extensions to the model are described in the next few sections. They involve partially activated FV (FV-h) and its interaction with FXa and TFPI α . The additional reactions describe the generation of FV-h, TFPI α binding to FV-h and FXa, direct inhibition of FV-h or FXa within prothrombinase by TFPI α , inhibition of FV-h:FXa prothrombinase assembly, and full activation of FV-h by thrombin. All of these additional reactions involving FV-h, FXa, and TFPI are sketched in Fig. 1 and listed in Table 1 with any available kinetic rate constants from the literature. In Eq. 1, we show the evolution equation for the concentration of one of the new species as an example of the nature of the model's equations. A full listing of the model equations and parameter values is given in the section S2 of [supporting material](#). Note that for this paper, the ordinary differential equations labeled 1–104 comprise the model. The remaining equations are added for the companion paper.

The model uses the following notation: Z_i and E_i to refer to a specific zymogen or pro-cofactor species and the corresponding enzyme or cofactor species when they are in the plasma, and Z_i^m and E_i^m refer to the surface-bound versions of these proteins (e.g., E_7^m refers to the TF:VIIa complex on the subendothelium, and E_5 and E_5^m refer to factor Va in the plasma and bound to a platelet surface, respectively). The new species, partially cleaved factor V is denoted E_5^d . The concentrations of the proteins are denoted similarly, but with lowercase z and e . Therefore, e_5^m is the concentration of platelet-bound factor Va. The symbols TF, P_2 , P_5 , P_8 , P_9 , P_{10} , and P_{11} are used to denote TF and the platelet binding sites for prothrombin, FV/FVa, FVIII/FVIIIa, FIX/FIXa, FX/FXa, and FXI, respectively. For the platelet binding sites specific to thrombin, factor IXa, and factor XIa, we use the symbols P_2^* , P_9^* , and P_{11}^* . The concentrations of binding sites are indicated similarly but with lowercase p . We denote the complex of Z_i and E_j by $Z_i : E_j$ and its concentration by $[Z_i : E_j]$, so, for example, $TFPI\alpha : E_{10}^m$ denotes $TFPI\alpha$ bound to platelet-bound factor Xa, and $[TFPI\alpha : E_{10}^m]$ refers to its concentration.

Generation and activation of FV-h

We assumed there are two major sources of FV-h: activation of FV by FXa (reaction 25 from [Table 1](#)) and secretion by platelets upon their activation. We assume here that FXa can only partially activate FV to FV-h. We also assume that a total of 3000 FV and FV-h molecules are released per activated platelet [\(33\)](#), and denote by h_5 the fraction of these which are FV-h molecules. For most of the simulations in this study we fixed $h_5 = 0.5$, but we also reported on simulations examining the model result's sensitivity to variations in h_5 . We assumed that FV and FV-h bind to the same platelet binding sites (P_5) and that platelet-bound FV-h and FXa can bind to one another to produce an early form of prothrombinase FV-h:FXa. We assumed that FV-h can be fully activated by thrombin, in the plasma, on the platelet surface, and within the FV-h:FXa complex (reactions 2, 6, and 9 in [Table 1](#)).

TFPI α binding to FV-h and FXa

In our previous model (23–25), TFPI α could bind only to fluid-phase FXa. Here, we also allowed TFPI α to bind directly from the plasma to platelet-bound Xa (reaction 22 in Table 1) and to FV-h in the plasma or bound to a platelet (reactions 1 and 5 in Table 1). We assumed that TFPI α cannot bind to FVa because the FV's B domain is completely removed upon full activation. This assumption is supported by the fact that TFPI binds FV in a form where only part of the B domain is cleaved upon activation by FXa, leaving the acidic region to bind the C-terminus of TFPI (13). We assumed that the entire 20% of plasma TFPI is the full-length form, which can interact with both FV-h and FXa. Differentiation between the truncated form and full-length forms of TFPI in the plasma is the subject for future research. Furthermore, we assumed that when FXa or FV-h is bound to TFPI α , it cannot subsequently form an FV-h:FXa prothrombinase complex. We based this assumption on the proximity of the binding sites on FV-h, FXa, and TFPI α for each other, the large size and flexibility of a TFPI α molecule, and the previous suggestion that this reaction is blocked (13,22,34). We do not consider the secretion of TFPI α from platelets in this model extension.

Direct inhibition of prothrombinase

We assume that prothrombinase is formed by the binding of platelet-bound FXa to platelet-bound FVa (FVa:FXa), as in our previous model, or to

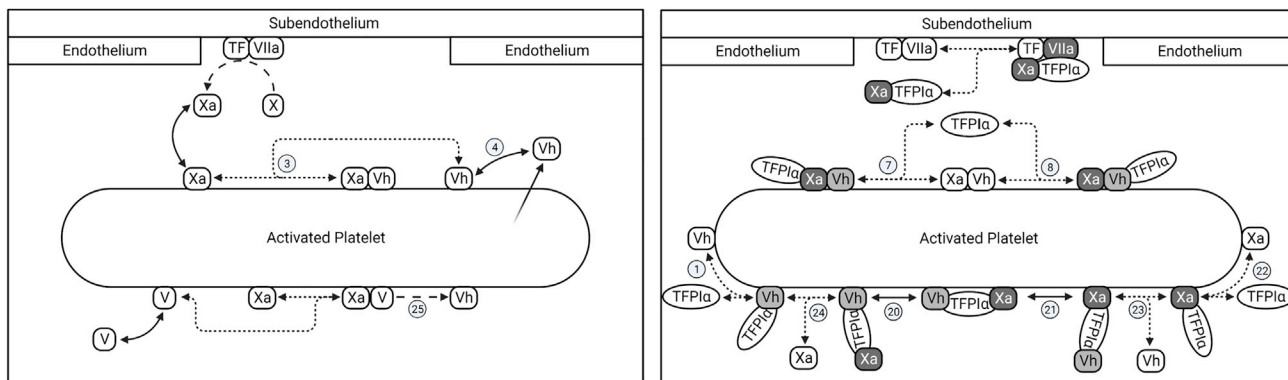


FIGURE 1 Newly added reactions involving FV-h, FXa, and TFPI α . (Left) Generation of FV-h through the activation of FV by FXa and secretion from platelet stores, binding/unbinding of coagulation factors to the platelet surface, and the assembly of prothrombinase. (Right) Binding of TFPI α to platelet-bound FXa, FV-h, and prothrombinase, and inhibition of prothrombinase assembly by TFPI α . Line styles indicate different interactions: dense dashed lines, binding and unbinding of protein pairs; longer dashed lines, catalytic reaction steps; solid double arrow, binding and unbinding of proteins with platelet surface; arrow with faded tail, secretion of protein from platelet. Light shade with black font indicates TFPI-bound and inhibited cofactors, and heavier shade with white font indicates TFPI α -bound and inhibited enzymes. FV is also secreted from platelet stores and can be activated by thrombin, but this is not shown because they were included in an earlier model. Circled numbers indicate reaction number listed in Table 1. To see this figure in color, go online.

TABLE 1 List of reactions added to the model and their kinetic rate constants, with literature references (k^+ shows forward reaction rate, k^- shows backward reaction rate, and k^{cat} indicates catalytic reaction rate)

Reaction list

Reaction no.	Reactants	Catalytic intermediate	Products	k^+ ($M^{-1} s^{-1}$)	k^- (s^{-1})	k^{cat} (s^{-1})	Note
1	$E_5^{hm} + \text{TFPI}$		$\text{TFPI}:E_5^{hm}$	$5.0(10)^7$	$4.5(10)^{-3}$		a
2	$E_5^{hm} + E_2^m$	$E_5^{hm}:E_2^m$	$E_5^m + EE_2^m$	$1.73(10)^7$	1	0.23	b
3	$E_5^{hm} + E_{10}^m$		$E_{10}^m:E_5^{hm}$	$1.0(10)^8$	0.01		c
4	$E_5^h + P_5$		E_5^{hm}	$5.7(10)^7$	0.17		d
5	$E_5^h + \text{TFPI}$		$\text{TFPI}:E_5^h$	$5.0(10)^7$	$4.5(10)^{-3}$		a
6	$E_5^h + E_2$	$E_5^h:E_2$	$E_5 + E_2$	$1.73(10)^7$	1.0	0.23	b
7	$E_{10}^m:E_5^{hm} + \text{TFPI}$		$\text{TFPI}:E_{10}^m:E_5^{hm}$	$1.6(10)^7$	$3.3(10)^{-4}$		e
8	$E_{10}^m:E_5^{hm} + \text{TFPI}$		$E_{10}^m:E_5^{hm}:\text{TFPI}$	$5.0(10)^7$	$4.5(10)^{-3}$		a
9	$E_{10}^m:E_5^{hm} + E_2^m$	$E_{10}^m:E_5^{hm}:E_2^m$	$E_{10}^m:E_5^m + E_2^m$	$1.73(10)^7$	1.0	0.23	b
10	$E_{10}^m:E_5^{hm} + Z_2^m$	$Z_2^m:E_{10}^m:E_5^{hm}$	$E_{10}^m:E_5^{hm} + E_2$	$7.13(10)^7$	1.0	27.5	f
11	$\text{TFPI}:E_5^{hm} + E_{10}^m$		$E_5^{hm}:\text{TFPI}:E_{10}^m$	$1.6(10)^7$	$3.3(10)^{-4}$		e
12	$\text{TFPI}:E_{10}^m + E_5^m$		$E_5^{hm}:\text{TFPI}:E_{10}^m$	$5.0(10)^7$	$4.5(10)^{-3}$		a
13	$\text{TFPI}:E_{10} + P_{10}$		$\text{TFPI}:E_{10}^m$	$1.0(10)^7$	0.025		d
14	$\text{TFPI}:E_5^h + P_5$		$\text{TFPI}:E_5^{hm}$	$5.7(10)^7$	0.17		d
15	$E_5^{hm} + \text{APC}$	$\text{APC}:E_5^{hm}$	$\text{APC} + E_{5,\text{dead}}^{hm}$	$1.2(10)^8$	1.0	0.5	g
16	$\text{TFPI}:E_{10} + E_5^h$		$E_5^h:\text{TFPI}:E_{10}$	$5.0(10)^7$	$4.5(10)^{-3}$		a
17	$\text{TFPI}:E_5^h + E_{10}$		$E_5^h:\text{TFPI}:E_{10}$	$1.6(10)^7$	$3.3(10)^{-4}$		e
18	$E_5^h:\text{TFPI}:E_{10} + P_5$		$E_5^{hm}:\text{TFPI}:E_{10}$	$5.7(10)^7$	0.17		d
19	$E_5^h:\text{TFPI}:E_{10} + P_{10}$		$E_5^h:\text{TFPI}:E_{10}^m$	$1.0(10)^7$	0.025		d
20	$E_5^{hm}:\text{TFPI}:E_{10} + P_{10}$		$E_5^{hm}:\text{TFPI}:E_{10}^m$	$1.0(10)^7$	0.025		d
21	$E_5^{hm}:\text{TFPI}:E_{10}^m + P_5$		$E_5^h:\text{TFPI}:E_{10}^m$	$5.7(10)^7$	0.17		d
22	$\text{TFPI} + E_{10}^m$		$\text{TFPI}:E_{10}^m$	$1.6(10)^7$	$3.3(10)^{-4}$		e
23	$\text{TFPI}:E_{10}^m + E_5^h$		$E_5^h:\text{TFPI}:E_{10}^m$	$5.0(10)^7$	$4.5(10)^{-3}$		a
24	$\text{TFPI}:E_5^{hm} + E_{10}$		$E_5^{hm}:\text{TFPI}:E_{10}$	$1.6(10)^7$	$3.3(10)^{-4}$		e
25	$Z_5^m + E_{10}^m$	$E_{10}^m:Z_5^m$	$E_5^{hm} + E_{10}^m$	$1.0(10)^8$	1.0	0.046	h

Notes: (a) Binding of TFPI α to FV-h, $K_D = 9$ pM from Jeremy et al. (15). (b) Activation of FV by thrombin, $K_M = 7.1(10)^{-8}$ M from Monković and Tracy (35). (c) Binding between FV-h and FXa, $K_D = 1(10)^{-10}$ M from Mann (36). (d) FV-h binding platelet surface, $K_D = 3(10)^{-9}$ M from Krishnaswamy et al. (37). (e) TFPI α binding FXa, $K_D = 2(10)^{-11}$ M from Jesty et al. (38). (f) Prothrombin activation by prothrombinase that has FV-h, $K_M = 0.4$ μ M from Petrillo et al. (20). (g) Inactivation of FV-h by activated protein C, $K_M = 12.5(10)^{-9}$ M from Solymoss et al. (39). (h) Generation of FV-h by FXa, $k_5^{cat} = 0.046$ s^{-1} and $K_M = 10.4(10)^{-9}$ M from Monković and Tracy (35).

platelet-bound FV-h (FV-h:FXa, reaction 3 in Table 1). Since FXa and FV-h can both be bound to TFPI α , via its Kunitz 2 domain and C-terminus region, respectively, we assume that FV-h:FXa can be directly inhibited by TFPI α binding either to FXa or to FV-h in the complex (reactions 7 and 8, respectively in Table 1). This is illustrated by the reactions shown on the top surface of the activated platelet in Fig. 1 (right). The binding kinetics for TFPI α binding to FXa or FV-h in the FV-h:FXa complex are considered to be the same as those for TFPI α 's binding to FXa or FV-h outside of the complex. Both forms of prothrombinase (FVa:FXa and FV-h:FXa) are assumed to be active and able to cleave prothrombin (20), but the enzymatic function of FV-h:FXa is assumed to stop when TFPI α is bound to either the FV-h or FXa part of the complex. TFPI α does not inhibit the enzymatic function of standard prothrombinase FVa:FXa.

Inhibition of prothrombinase assembly

As mentioned above, we assume that TFPI α can be bound to both FXa and FV-h at the same time via its Kunitz 2 domain and C-terminus, respectively, but binding interactions between FXa and FV-h in that case are blocked. In this situation, TFPI α is inhibiting the assembly of FXa and FV-h into prothrombinase. The inhibition of assembly can occur through two different, two-step reactions: TFPI α binds to FV-h via its C-terminus first and then binds to FXa via its K2 domain (reaction 11

in Table 1), or TFPI α binds to FXa via its K2 domain first and then binds to FV-h via its C-terminus (reaction 12 in Table 1). This is illustrated by the reactions shown on the bottom surface of the activated platelet in Fig. 1 (right). Each coagulation factor to which TFPI α is bound can either be platelet bound or in the fluid. Thus, there are multiple situations to consider, including ones in which one of the coagulation factors in the FV-h: TFPI α :FXa complex is bound to the platelet membrane and the other factor is not bound to the membrane, but is held close to the platelet through its interaction with TFPI α (reactions 16–21 in Table 1). In such cases, the free end of the ternary complex can become attached to the membrane, or the membrane-bound end can detach from the surface and release the entire ternary complex into the fluid. The fluid-phase ternary complex can rebind to a platelet surface by either its FV-h or FXa, or it may be washed away by the flow.

Model equations

The reactions in Table 1 are translated into mathematical equations using the law of mass action. Equation 1 is an example of the type of equations that constitute the model. It describes the rate of change of the concentration of FV-h in the fluid by the processes of the binding and unbinding of FV-h from the platelet surface, its delivery or removal due to flow, its secretion from the platelet, its full activation by thrombin, and its binding to and unbinding from TFPI α :

$$\begin{aligned}
\frac{de_5^h}{dt} = & \underbrace{-k_5^{\text{on}} e_5^h p_5^{\text{avail}}}_{\text{FV - h binding to platelet}} + \underbrace{k_5^{\text{off}} e_5^h m}_{\text{FV - h unbinding from platelet}} \\
& + \underbrace{k_{\text{flow}}(e_5^{h,\text{up}} - e_5^h)}_{\text{FV - h flowing in/away from RZ}} \\
& + \underbrace{h_5 \cdot n_5 \cdot \frac{d}{dt} ([PL_a^s] + [PL_a^v])}_{\text{FV - h secretion term}} \\
& - \underbrace{k_{e_5^h; e_2}^+ e_2 e_5^h}_{\text{binding of FV - h to thrombin}} \\
& + \underbrace{k_{e_5^h; e_2}^+ [E_5^h : E_2]}_{\text{dissociation of FV - h from thrombin}} - \underbrace{k_{e_5^h; \text{TFPI}}^+ e_5^h \cdot \text{TFPI}}_{\text{TFPI binding FV - h}} \\
& + \underbrace{k_{e_5^h; \text{TFPI}}^+ [E_5^h : \text{TFPI}]}_{\text{TFPI unbinding FV - h}}. \tag{1}
\end{aligned}$$

In this equation, p_5^{avail} denotes the concentration of platelet binding sites for FV, FV-h, and FVa that are not already bound to one of these species, n_5 denotes the total number of FV and FV-h molecules released by a platelet when it is activated, $e_5^{h,\text{up}}$ is the concentration of FV-h in the bulk plasma (generally set to 0), and $\frac{d}{dt}([PL_a^s] + [PL_a^v])$ is the rate at which platelets are activated. The other quantities are defined in Table 1.

RESULTS

Tissue factor and shear rate dependency

Here we examined how the variation in TF density and shear rate affected thrombin production with the additional TFPI α inhibitory mechanisms and compared the outcomes with those from our previous model. We focused on how TF and shear rate dependency differ for low (0.5 nM) and high (2.5 nM) TFPI α plasma concentrations. For various TF densities in the range 0–20 fmol/cm² and for shear rates 100/s, 500/s, and 1500/s, we performed simulations with the old and new models. We looked at two output metrics: the lag time, which we define as the time point at which the thrombin concentration first reaches 1 nM, and the thrombin concentration at 10 min. Fig. 2, A and C show the lag times and Fig. 2, B and D show the thrombin concentrations at 10 min. For both old and new models and for both TFPI α levels, the lag time decreased as the TF density increased and/or the shear rate decreased. The reason for these behaviors is that a higher TF density provides a larger initial stimulus and decreasing the shear rate slows the loss of essential enzymes from the RZ. Also, the thrombin concentrations at 10 min increased with the TF density, sharply at low TF densities and more gradually at high ones. In fact, the results indicated a threshold dependence on TF density in all cases examined. (We refer to curves of thrombin at 10 min versus TF density as threshold curves.) The thrombin concentration at 10 min was also affected by the shear rate; in particular,

the level of TF necessary to achieve a high thrombin concentration depended on the shear rate and, for high TF, the thrombin concentration at 10 min was somewhat higher for lower shear rate.

In Fig. 2, results for the old and new models are indicated by gray and black lines, respectively. In Fig. 2, A and C we see that, for a given TF density, the newly added TFPI α inhibition increases the lag time, and that to achieve a particular lag time a larger TF density was needed with the new model. This is because the additional inhibition reactions made it more difficult for the system to accumulate FXa on platelet surfaces, and this slowed prothrombinase formation and thrombin generation. We see for both TFPI α levels that the change in lag time between the two models was greater at higher shear rate. For the low TFPI α level (Fig. 2 A), we see that for each shear rate, the curves for the two models converged as the TF density was increased, indicating that the effect of the additional inhibition is more pronounced at low TF densities. Compared with these results, we see that for the higher TFPI α level (Fig. 2 C), the differences between the two models were greater for each TF density and that a substantial effect of the additional inhibition persisted to much higher TF densities.

Turning to Fig. 2, B and D, we look at how the thrombin concentration at 10 min differs between the two models for different TF densities and shear rates. For each shear rate, the threshold TF density was increased by the additional TFPI α inhibition reactions, that is, the threshold curves were shifted to the right. For low TFPI α , the effect was small for shear rate 100/s and progressively increased as the shear rate was increased first to 500/s and then to 1500/s. For the range of TF densities that were above threshold for the old model and below threshold for the new one, there was a notable difference in the thrombin concentrations at 10 min. For TF densities that were below threshold for both models or above threshold for both models, there was little effect of the additional inhibition reactions. In particular, at high TF densities the thrombin concentrations at 10 min are very similar. For high TFPI α , the effects of the model changes are more dramatic. There is a much broader range of TF densities which for the old model are above threshold and for the new model are below threshold, and for TF in this range there was a substantial difference in the thrombin concentrations achieved with the two models.

In summary, a major effect of the additional platelet-surface-mediated TFPI α inhibition reactions was to increase the TF threshold for substantial thrombin production to a degree that increased with increasing plasma TFPI α levels. For TF densities that were above threshold for both models, the lag time was larger with the additional reactions. The magnitude of the extra delay in thrombin production engendered by the additional inhibition varied with the TF density and shear rate and was substantial for a range of TF densities and shear rate 1500/s for low TFPI α and for a much broader range of TF densities and all shear rates considered for high

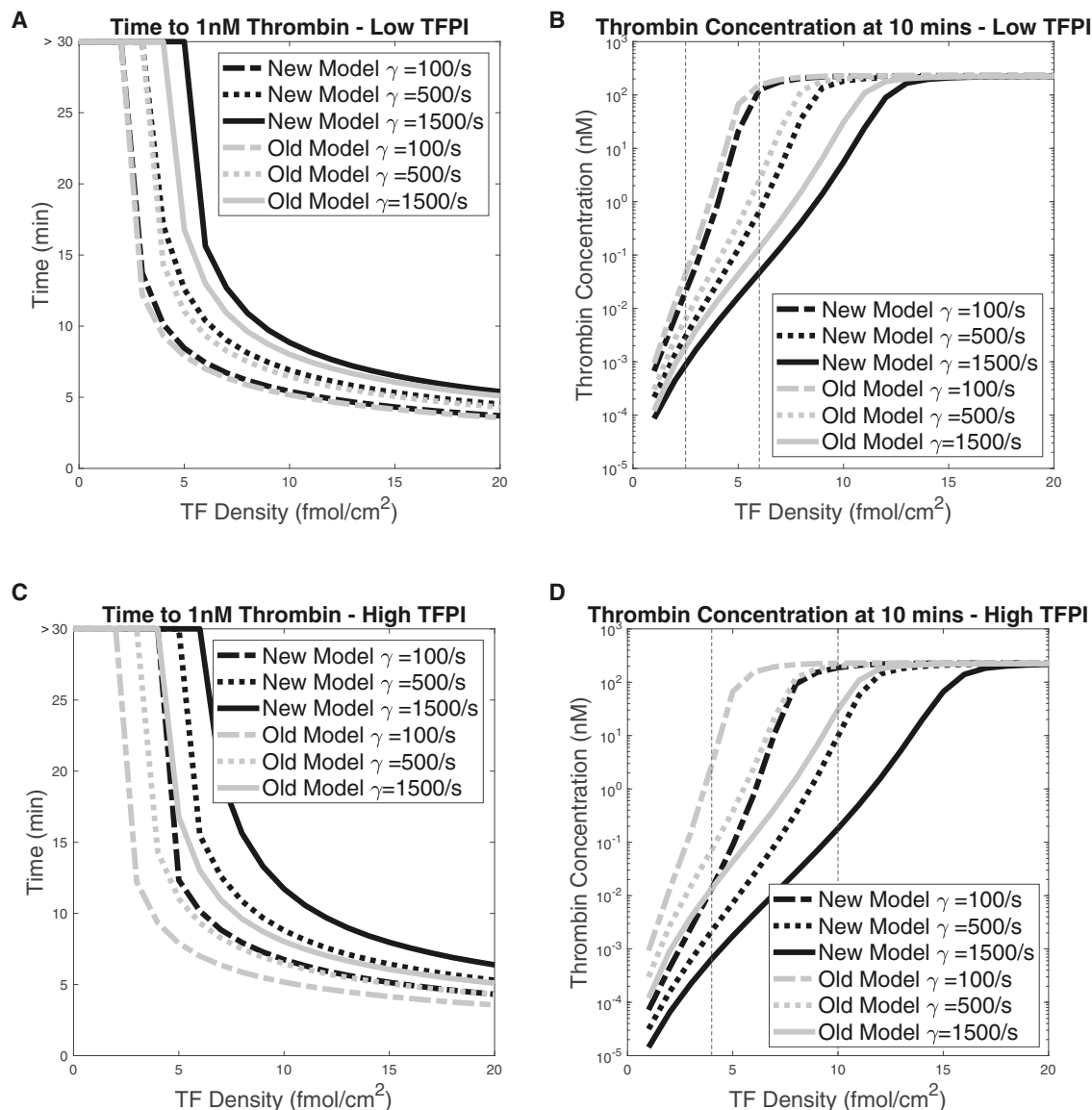


FIGURE 2 Effects of the TF level and shear rate on the lag time and the thrombin concentration after 10 min for a range of TF densities and three different shear rates. Black curves represent the results from the new model, which includes the additional TFPI α -mediated inhibition reactions, and gray curves represent the results from the old model, where TFPI α could only bind to fluid-phase FXa and then to TF:VIIa. All simulations were run with $[TFPI\alpha] = 0.5$ nM. Vertical dashed lines in (A) and (C) at lag time >30 indicate that the thrombin concentration did not reach 1 nM within 30 min for the corresponding TF density.

TFPI α . The thrombin after 10 min for a sufficiently high TF density was affected little by the additional reactions for both TFPI α levels and all shear rates considered.

Impact of TFPI α concentration on thrombin generation

The previous results were based on variations in TF and shear rate for two fixed plasma concentrations of TFPI α . Next, we fixed the TF density at 2.5 fmol/cm² or 10 fmol/cm² and the shear rate at 100/s, and studied how varying the TFPI α levels from 0 to 2.5 nM in increments of 0.5 nM affected thrombin generation. We did this only

with the new model, as the old model's results varied negligibly with the TFPI α level. The variation of thrombin with time for these experiments is shown in Fig. 3. In Fig. 3 A, two qualitatively different outcomes are seen for a TF density of 2.5 fmol/cm² depending on the TFPI α level. As the TFPI α concentration was increased from 0 nM to 0.5 nM and then to 1.0 nM, there was a substantial prolongation of the lag time from 923 s to about 1400 s to about 1980 s. The thrombin concentrations at 40 min in these simulations were 333, 303, and 261 nM for TFPI α concentrations of 0, 0.5, and 1.0 nM, so the new inhibition reactions also affected, albeit modestly, the thrombin concentrations at this time. For higher TFPI α concentrations (1.5, 2.0, and

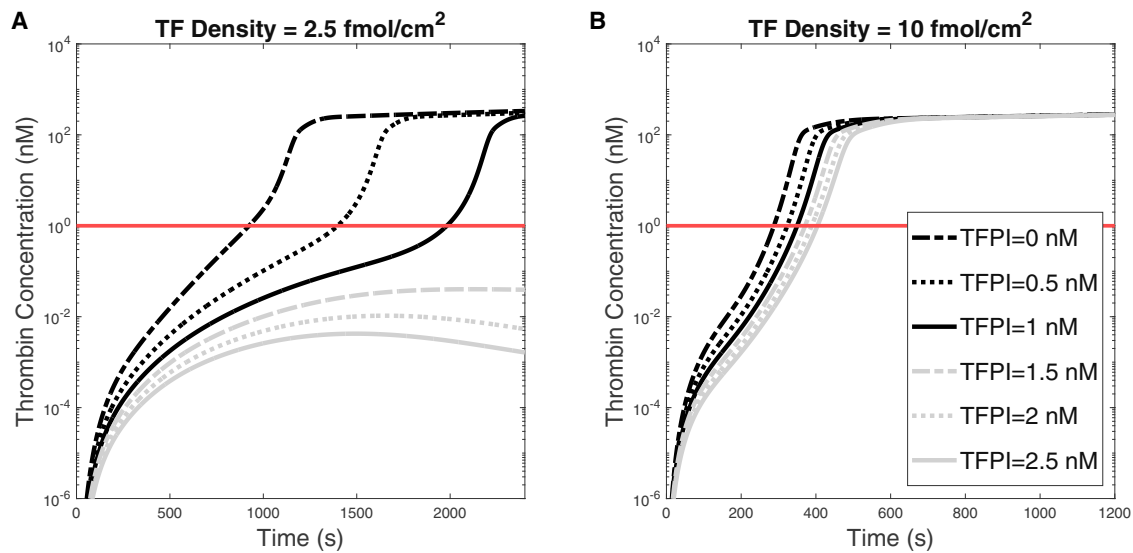


FIGURE 3 Thrombin concentration versus time for the indicated $\text{TFPI}\alpha$ levels for shear rate 100/s and with (A) $\text{TF} = 2.5 \text{ fmol}/\text{cm}^2$ and (B) $\text{TF} = 6 \text{ fmol}/\text{cm}^2$. Note the different timescales. To see this figure in color, go online.

2.5 nM) the thrombin curves peaked at levels below 1 nM and were in decline during the latter part of the simulations, indicating that robust thrombin production would never occur. These results are reflected in and explained by the concentration time course of FXa, FV-h, and their complexes with $\text{TFPI}\alpha$ under different TF, shear rate, and TFPI levels, as shown in Fig. S7. Similar to what we observed for thrombin, higher TF levels lead to higher concentrations of platelet-bound FXa and FV-h, whereas responses to increases in shear rate are more sensitive at low TF levels (see Fig. S7).

The thrombin curves for a TF density of 10 fmol/cm² are shown in Fig. 3 B. At this TF density, the variations in $\text{TFPI}\alpha$ levels prolonged the lag time modestly and robust thrombin production occurred for all the $\text{TFPI}\alpha$ concentrations examined. These results reinforced our earlier observation that the additional $\text{TFPI}\alpha$ -mediated inhibition reactions can strongly influence thrombin dynamics with the greatest impact occurring for low TF densities. These results are in line with experimental ones showing that the major inhibitory effects of TFPI under flow occur at low TF (40). In that study, Thomasen et al. showed that TFPI antagonism decreases the lag time of fibrin deposition at low TF and to a lesser extent at higher TF levels. Our results for thrombin generation with $\text{TFPI} = 0$ and 0.5 nM, plotted on a linear scale (Fig. S4), compare well with their time courses of fibrin deposition and differences they see in lag times with and without TFPI antagonism and under different TF levels.

Examination of the major inhibitory reaction step(s)

Our model included two new ways that TFPI could impede thrombin generation: through direct binding with platelet-

bound FXa and through interactions with FV-h. To investigate whether one binding reaction more greatly affects the lag time and to determine for which TF levels that occurred, we computed the lag times as we varied the TF density and the $\text{TFPI}\alpha$ concentration with and without the binding of $\text{TFPI}\alpha$ to FXa and FV-h. The results are shown in the four heatmaps in Fig. 4. In the heatmaps, the color indicates the lag time in minutes (white cells indicate that the thrombin concentration did not achieve 1 nM within 40 min), a minus sign indicates that the binding reaction is “turned off,” and a plus sign indicates that the binding reaction is “turned on.” To “turn off” the binding of $\text{TFPI}\alpha$ to FXa, we set all association rates between $\text{TFPI}\alpha$ and FXa to zero (reactions 7, 11, 17, 22, and 24 in Table 1). Similarly, to “turn off” $\text{TFPI}\alpha$ binding with FV-h, we set all association rates between TFPI and FV-h to zero (reactions 1, 5, 8, 12, 16, and 23 in Table 1).

As expected, when we turned off $\text{TFPI}\alpha$ binding to both FXa and FV-h, shown in Fig. 4 A, we observed that the lag time was dependent only on TF (displaying threshold dependence) and was independent of the $\text{TFPI}\alpha$ concentration. For simulations in which we turned on only the binding between $\text{TFPI}\alpha$ and FV-h, the lag time exhibits dependence on $\text{TFPI}\alpha$, but this effect saturated at a $\text{TFPI}\alpha$ concentration greater than about 3 nM (Fig. 4 B). Also, the influence of the $\text{TFPI}\alpha$ concentration on the lag time was much diminished for TF densities higher than about 6 fmol/cm².

If instead we turned on only the binding of $\text{TFPI}\alpha$ to FXa, there was a slightly greater dependence of lag time on both $\text{TFPI}\alpha$ and TF, and this effect did not saturate with $\text{TFPI}\alpha$ level, at least up to 5 nM (Fig. 4 C). Turning on both binding reactions, as seen in Fig. 4 D, the lag time threshold was shifted to a higher TF level than in either of the previous cases, consistent with the shift in

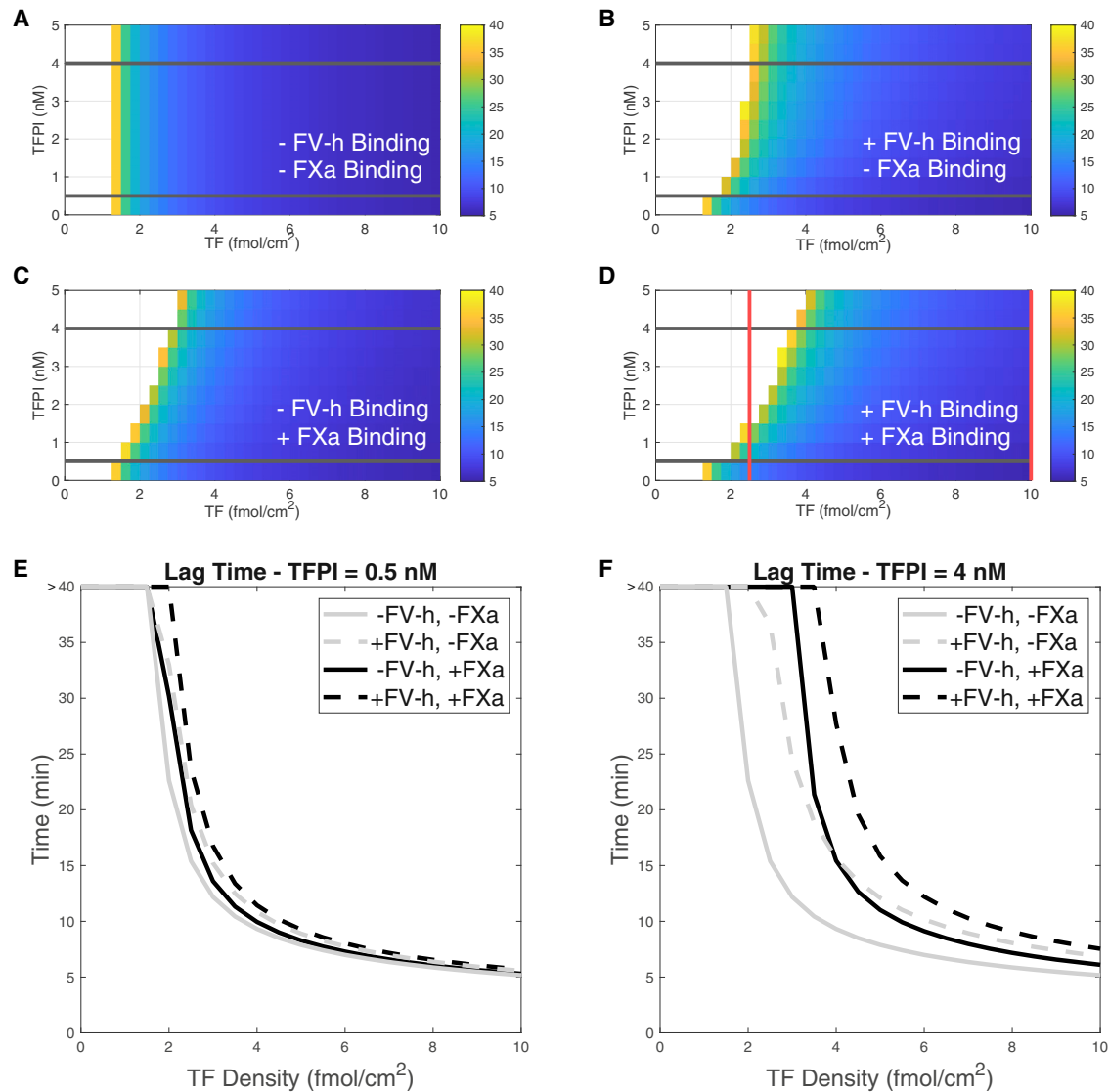


FIGURE 4 Lag times as functions of TF and TFPI α levels with the specified TFPI α binding reactions. Lag times for cases in which (A) TFPI α binding with both FV-h and FXa are turned off, (B) TFPI α binding with FV-h is turned on and TFPI α binding with FXa is turned off, (C) TFPI α binding with FXa is turned on and TFPI α binding with FV-h is turned off, and (D) TFPI α binding to both FV-h and FXa are turned on. For parameter values in the region without color, the thrombin concentration did not reach 1 nM thrombin within 40 min. Lag time versus TF density for TFPI α = 0.5 nM with and without TFPI α binding FV-h or/and FXa for (E) TFPI α = 0.5 nM and (F) TFPI α = 4.0 nM. These curves correspond to the slices in the heatmap indicated by the horizontal lines in (A)–(D). Shear rate is fixed to 100/s. To see this figure in color, go online.

the TF threshold in the new model revealed in Fig. 2. Note also that the red vertical line at TF 2.5 fmol/cm² represents the same information as that at the intersections of the thrombin curves and the 1 nM level line (*red horizontal line*) in Fig. 3, where the TF density was fixed to 2.5 fmol/cm². Comparing the heatmaps in Fig. 4, B and C, we conclude that binding of TFPI to one of either FV-h or FXa significantly altered the lag time but that the TFPI α -FXa binding had a stronger influence.

For a more detailed comparison of the lag times for the four cases at specific TFPI levels, Fig. 4, E and F show plots of the lag times as a function of TF density for two specific TFPI α concentrations, 0.5 nM and 4 nM, indicated with hor-

izontal black lines in the heatmaps. These plots allow a clearer comparison of the effects of each of the binding reactions on lag times. In particular, Fig. 4 E shows that at the lower TFPI α , lag times are increased in the order of adding TFPI α /FV-h reactions alone, adding TFPI α /FXa reactions alone, and finally both reactions together (the curves shift slightly to the right and never cross). However, for the higher TFPI α shown in Fig. 4 F, the larger lag times are clearer but, additionally, a larger effect of one of the individual reactions alone depends on the TF density (*gray dashed line* and *black solid line* cross at TF 4 fmol/cm²). The greatest increase in lag time occurred when both reactions were at play (Fig. 4 D).

Significance of platelet-derived FV

To further investigate the importance of FV-h in the coagulation system, we explored the effect of the FV-h derived from platelets that is secreted upon activation. We did this by varying the parameter h_5 that denotes the fraction of all of the FV-type molecules released by the platelet that are half-activated FV-h. This parameter is used in Eq. 1. Fig. 5 shows the thrombin generation over time for various h_5 and TF values for low (0.5 nM) and high (2.5 nM) TFPI α plasma concentrations. We vary h_5 among 0, 0.5, and 1, which correspond, respectively, to only zymogen FV, a mixture of half FV, and half partially activated FV-h, and only FV-h being released from platelets upon activation. At the low TFPI α concentration, we considered TF densities 2.5 and 6.0 fmol/cm 2 and for the high TFPI α concentration, we ran simulations at TF densities 4.0 and 10.0 fmol/cm 2 . These values, indicated by vertical lines in Fig. 3, B and D, bracket the range of TF values over which the thrombin concentration at 10 min changed rapidly as the TF density was varied for shear rate 100/s and the low and high TFPI α concentrations, respectively.

For both TFPI α concentrations, the resulting behaviors were qualitatively similar but differed in magnitude. In Fig. 5 A, we see that for TFPI α = 0.5 nM and for the higher TF density (6.0 fmol/cm 2), there was little difference in the thrombin curves for the different h_5 values. In contrast, for the lower TF density (2.5 fmol/cm 2), the effect of increasing h_5 was to shorten the lag time, from 1419 s when only zymogen is released by the platelets, to 1080 s for the 50:50 mixture, to 914 s when only partially activated FV-h was released. For both TF densities, the thrombin concentration at 40 min changed little with changes in h_5 . Fig. 5 B shows that for TFPI α = 2.5 nM, there was almost negligible

difference in the thrombin curves for the higher TF density (10.0 fmol/cm 2) and that, while the variation in lag time with h_5 was greater for TF density (4.0 fmol/cm 2), it was much less than for the combination of low TFPI α concentration and low TF density shown by the black curves in Fig. 5 A. To summarize, an increase of FV-h content within the platelets shortened the lag times. When TFPI α was low, the effect was the greatest for a low TF density.

Local sensitivity analysis

We performed a local, one-at-a-time, sensitivity analysis (SA) of the new model to the new parameters relating to TFPI binding with FV-h. All of the details and the results are shown in the section 4 of the [supporting material](#) and in Figs. S2 and S3, and we will give only a brief summary of them here. The SA methods were based on those developed by Saltelli and colleagues (41,42) and those we used to analyze our previous model (27). We chose three thrombin metrics: lag time, maximum rate of thrombin generation, and final thrombin concentration, as the quantities of interest and then ranked the sensitivities of these quantities to levels of all clotting factors and inhibitors except for TFPI α , as in our previous work (27). The lag times in the new model showed a higher sensitivity to TFPI α levels than in our old model, as expected from the previous results shown above; the effects of TFPI α on the maximum rates and final thrombin concentration were negligible, as they were with the previous model. However, in comparison with our previous SA results, FX became increasingly important for the lag times and maximal rates with the new model, which makes sense given the direct inhibition of FXa on platelet surfaces by TFPI α . Next, a local SA

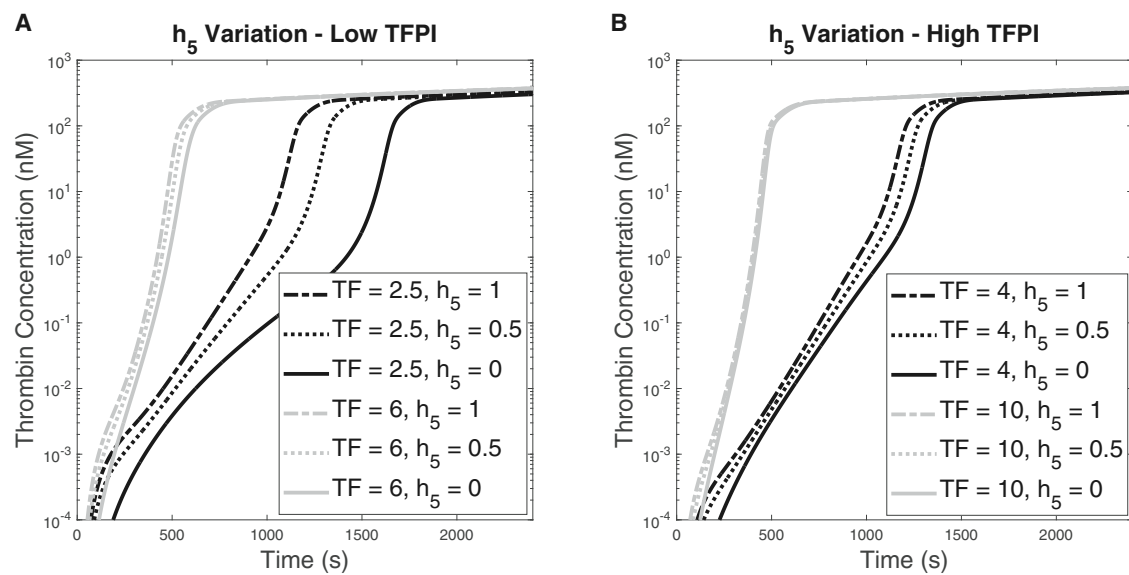


FIGURE 5 Thrombin generation for $h_5 = 0, 0.5, 1.0$ for shear rate 100/s. (A) The TFPI α concentration is 0.5 nM and the TF density was either 2.5 or 6 fmol/cm 2 . (B) The TFPI α concentration is 2.5 nM and the TF density was either 4 or 10 fmol/cm 2 .

was performed on the kinetic rates. Forward and reverse kinetic rates for each of the $\text{TFPI}\alpha/\text{FV-h}$ reactions were varied by 10%, and the changes in the three thrombin metrics were measured. These small perturbations in reaction rates had minimal effects on all thrombin metrics; none of the perturbations led to more than a 1% change from baseline metric values.

DISCUSSION

Our previous mathematical model, in which $\text{TFPI}\alpha$ acts only through FXa and TF:VIIa , showed minor inhibitory effects of $\text{TFPI}\alpha$ on thrombin generation. In that model, most FXa that was produced on the subendothelium and subsequently bound to $\text{TFPI}\alpha$ in the fluid was quickly washed away by the flow before it could rebind to the TF:VIIa in the small injury zone. It is possible that for a longer injury, the fluid-phase $\text{FXa:TFPI}\alpha$ complexes might bind to TF:VIIa downstream and inhibit its action. Other reaction schemes for this pathway have been considered (24,38,43–45), which has led to some disagreement regarding the effects of $\text{TFPI}\alpha$ under flow. Further mathematical investigation of different schemes and injury sizes is warranted to better understand $\text{TFPI}\alpha$ inhibition via TF:VIIa under flow.

To the best of our knowledge, the current study is the first mathematical modeling approach to investigate $\text{TFPI}\alpha$ inhibition on the surface of activated platelets. We extended our previous model to include generation and activation of FV-h as well as its inhibition by $\text{TFPI}\alpha$ on activated platelet surfaces. Additionally, we included $\text{TFPI}\alpha$ binding to FXa bound to an activated platelet surface that leads to its inhibition. These extensions relate solely to platelet-surface reactions, and essentially all of the inhibitory effects of $\text{TFPI}\alpha$ we observe in the extended model are due to these reactions, since $\text{TFPI}\alpha$ had very little influence in our earlier model. We studied how the newly added $\text{TFPI}\alpha$ inhibition pathways affected thrombin generation related to the TF threshold behavior, thrombin lag times, the system's sensitivity to shear rate, and how thrombin generation was affected by varying $\text{TFPI}\alpha$ levels at low and high TF densities. In general, we found that the newly added $\text{TFPI}\alpha$ reactions created a new sensitivity of the model system to $\text{TFPI}\alpha$ levels, especially at low TF levels. At high TF densities, the same $\text{TFPI}\alpha$ concentration increased the lag time but still led to a robust thrombin response. In fact, when a strong thrombin response was generated, under variations of $\text{TFPI}\alpha$ from 0 to 5 nM, the system produced approximately the same final thrombin concentrations.

Our general results about $\text{TFPI}\alpha$ inhibition under flow are in line with previous experimental studies performed with microfluidics (40). In those studies, it was observed that $\text{TFPI}\alpha$ antagonism enhanced fibrin formation (thrombin generation in our model can be thought of as a surrogate for fibrin formation) when normal blood or plasma was

flowed over TF/collagen microspots, but this effect was seen only at low TF densities. The experiments did not run long enough to find out whether the final fibrin fluorescence achieved was similar with and without $\text{TFPI}\alpha$ antagonism; however, there was a significant fibrin response that was delayed with $\text{TFPI}\alpha$. Taken together with our results, this suggests that platelet-surface-dependent $\text{TFPI}\alpha$ inhibition affects the timing but not the magnitude of a thrombin response and that these effects are most pronounced at low TF densities. TFPI leads to delayed lag times under static conditions as well. van't Veer and Mann performed thrombin generation assays with and without TFPI and with varying levels of TF (46). In comparing the lag times with TFPI with those without, they found that it was always increased and that the increases were more prominent for lower TF levels. Although these assays were performed with lipid vesicles and not platelets, the surface-dependent mechanism could still be at play.

Our mathematical model gives as output the concentration of every model species at every point in time, and also gives us the freedom to turn on and turn off specific pathways. These capabilities allowed us to investigate $\text{TFPI}\alpha$ binding with FXa and FV-h to characterize their individual and combined inhibitory behavior. In turning off these pathways separately and together, we found that $\text{TFPI}\alpha$ binding with both FXa and FV-h has a strong inhibitory role. When $\text{TFPI}\alpha$ could bind with FV-h but not with FXa in either plasma or on platelet surfaces, the inhibitory effect of $\text{TFPI}\alpha$ saturated at about a 3 nM $\text{TFPI}\alpha$ concentration. With the FXa inhibition pathway on but without $\text{TFPI}\alpha/\text{FV-h}$ binding, the inhibitory effects of $\text{TFPI}\alpha$ increased with increasing $\text{TFPI}\alpha$ concentration up to the maximum that we simulated (5 nM). These results can be explained by considering what constitutes prothrombinase in the system. In this new model, there are two forms of prothrombinase, FXa:FV-h and FXa:FVa , both of which can actively convert prothrombin to thrombin. In our model, to form either type of prothrombinase complex, FV must first be converted to FV-h by FXa or to FVa by thrombin. Only FXa is present in the initial stage of coagulation, so FV-h is available first. This allows formation of FV-h:FXa , which generates the first thrombin. Once a sufficient level of thrombin is reached, thrombin becomes the primary activator of FV , fully activating it to FVa and leading to FXa:FVa formation, which is protected from $\text{TFPI}\alpha$ inhibition and further supports propagation of thrombin. This is in line with the proposed scheme of Schuijt et al. (14) suggesting that FXa -dependent FV activation is pivotal to the initiation phase of coagulation. Essentially, FV-h is needed early to generate the first thrombin and start the positive feedback, then FVa is the primary cofactor for FXa . In other words, the prothrombinase concentration is limited by the amount of FXa and not by the amount of FV-h , and this explains the observed differences between the two inhibitory pathways.

The composition of platelet-released FV forms was important in the new model. Increasing the amount of FV-h relative to FV within the platelets resulted in acceleration of thrombin generation, with the most significant effects at low TF and effects that are mostly washed out at higher TF. At low TF, if all platelet-released FV was FV-h there would be no need for FXa to activate it first, thus removing a reaction step and accelerating coagulation. Additionally, the released FV-h would be able to immediately bind to FXa on activated platelet surfaces to form active prothrombinase (FV-h:FXa) during the early stages of coagulation. Our simulations in this study were performed under the assumption of normal healthy blood, and it is possible that these effects are magnified in the case of hemophilia A. In our previous study (28), in which the model did not account for FV-h, we found that lowering the FV levels in plasma and platelets could enhance thrombin generation in hemophilia A, where there is a deficiency in FVIII. In that study, the model suggested that the reason for this is that FV and FVIII compete for FXa in the early stage of coagulation and that lowering FV weakens this competition so that more of the albeit small quantity of FVIII can be activated; this leads to more tenase, more prothrombinase, and ultimately to more thrombin. In our new model we have introduced a new species that also competes for FXa, namely FV-h. Thus there is now competition between three species for FXa: FV, FVIII, and FV-h. It will be interesting to see how this changes our results for hemophilia A blood, and this is a topic of immediate future research.

It seems plausible, then, that a reduction or modulation of inhibitors could offset complications associated with bleeding disorders. For example, TFPI α levels have been shown to affect clotting in individuals with hemophilia A and B, the bleeding disorders characterized by deficiencies in clotting factors VIII (FVIII) and IX (FIX), respectively. Several biochemical experiments have revealed relationships between TFPI α and the early stages of coagulation in hemophilia blood (47). One study showed that TFPI α modulates the generation of FXa by inhibiting TF:VIIa in the presence of FVIII and FIX (48), suggesting that TFPI α itself could be inhibited to enhance coagulation. This hypothesis was examined in various animal models as well: a recent mouse study demonstrated that an anti-TFPI α antibody used in mice under hemophilic conditions decreased the hemoglobin lost over 20 min following tail transection. This indicated that direct inhibition of TFPI α effectively suppressed tail bleeding in mice with hemophilia (49). Another study showed that rabbits made temporarily hemophilic with anti-FVIII antibodies had reduced mean bleeding times after injection with anti-TFPI α antibodies (50). This study demonstrated that partial inhibition of TFPI α mitigates bleeding under hemophilia conditions. Together with our previous findings regarding FV and hemophilia, these studies suggest the potential for TFPI α and FV manipulation in the treatment of hemophilia. Further inves-

tigation of interactions between TFPI α and FV and their effects on coagulation in hemophilia is thus warranted. As a first step, we have developed a mathematical model of coagulation under flow that includes the relevant TFPI α and FV interactions with the goal of making possible future studies focused on hemophilia.

The reason we studied TFPI α at 0.5 and 2.5 nM is because it is still not clear how much free TFPI α is in the blood. Although TFPI is often reported to be 2.5 nM in plasma, TFPI α has been suggested to account for only 10%–30% of the total TFPI pool in the blood (15), with platelet TFPI accounting for about 7%–8% of this total (5). Approximately 80% of plasma TFPI is a C-terminus truncated form (cannot bind to FV-h) and is thought to be bound to lipoprotein (51). Although one biochemical study showed that the lipoprotein-bound form of TFPI can actively inhibit thrombin generation (52), it is not entirely clear how inhibitory this form is *in vivo*. The remaining 20% is free in the plasma and consists of a mixture of a full-length TFPI α form and the truncated form. Thus, the 0.5 nM levels studied here represent that 20%.

One limitation of our model is the absence of explicit inclusion of protein S in the coagulation reactions. Protein S is known to be a critical regulator of coagulation, playing the role of cofactor for both activated protein C and TFPI α in the inactivation of FVa and inhibition of FXa, respectively (53). Protein S can bind directly to lipid surfaces, and thus could localize TFPI α bound to the protein S near the lipid surface. This is likely part of a mechanism that enhances the rate of encounter between platelet-bound FXa and TFPI α . FV-short and protein S have recently been shown to be synergistic cofactors for TFPI α , leading to much stronger inhibition of FXa together than when TFPI α is bound to only one of FV-h or protein S (54). This synergy seems to occur via formation of a trimolecular complex of TFPI α , FV-short, and protein S (55, 56), and it was hypothesized that these complexes are present in circulating plasma at subnanomolar concentrations (56). Considering the high concentrations of protein S in plasma, it was further suggested that nearly all of the TFPI α in plasma may be bound within such trimolecular complexes and that no or very little free FV-short or free TFPI α exists in plasma (55). However, data supporting that hypothesis are sparse and, as mentioned above, it is still unclear how much free TFPI α exists in circulating plasma. While we do not include protein S explicitly in our model, some of our simulation results may still shed light on its potential effects. For example, our simulations with high levels of plasma TFPI α can be thought of as corresponding to lower levels of the protein S-FV short-TFPI α complex which has 10-fold higher power to inhibit FXa than does TFPI α alone (53). Similarly, if almost all plasma TFPI α is in complex with protein S and FV-short, little TFPI α would be available to bind with FV-h produced by FXa or released from platelets, while FXa-inhibiting capability would still be present. Our simulations in

which we “turned off” TFPI α binding to FV-h would correspond, at least approximately, to that situation. Thus, even in scenarios in which TFPI α circulates in complex with protein S and FV-short, our model provides strong evidence that direct inhibition of platelet-bound FXa is an important mechanism for regulating thrombin generation under flow. In future research, we plan to explicitly include in the model protein S and its cofactor activity for TFPI α and activated protein C.

Finally, it is also known that platelets secrete TFPI α upon activation with thrombin (5,57). The exact location of these TFPI α molecules within the platelet is unknown, but it is known that it is not the α -granules (57) where FV is stored. It is possible that this stored and released TFPI α pool could play an important role in regulating thrombin generation, especially if protein S can quickly localize it to the platelet surface. This is another topic of immediate future research.

CONCLUSION

In this study, we extended a mathematical model of flow-mediated coagulation to explore the effects of TFPI α -mediated inhibitory reactions that take place on activated platelet surfaces. Results from our new model show that the surface-dependent TFPI inhibition is much stronger than the TFPI inhibition on the subendothelium and, as such, the TF threshold density is shifted to higher values in our new model compared with our old one. Furthermore, these reactions could lead to significant delays in thrombin generation at low TF density if TFPI α levels were increased. Ultimately, the new model was sensitive to changes in TFPI α levels, especially at low TF density, and gave TFPI α potential to be a significant modifier of thrombin generation. There are still some additional limitations in this model that we need to address in future work: 1) we do not include TFPI α secretion from platelets; 2) we do not consider inhibition by TFPI β in the endothelial region; and 3) some reaction kinetics are unknown and we thus made assumptions about their values, and more experimental data would be useful for defining more precise values. Nevertheless, we developed an updated version of an experimentally validated mathematical model of flow-mediated coagulation that is sensitive to TFPI α and successfully exhibits the experimentally observed inhibitory effects of TFPI α under flow. More importantly, this model revealed the importance of the platelet surface as a platform for efficient inhibition. It is known that the platelet-surface dependence of procoagulant enzyme reactions is key to localizing coagulation to the site of injury. Thus, it makes sense that the inhibition of these key enzymes should also be most effective where they are needed most. Finally, TFPI α may be a potential therapeutic target to rescue thrombin generation in various bleeding disorders, and the current model can serve as a foundational tool to assess the effectiveness of TFPI α as a modifier of thrombin generation in these cases.

SUPPORTING MATERIAL

Supporting material can be found online at <https://doi.org/10.1016/j.bjpi.2022.11.023>.

AUTHOR CONTRIBUTIONS

K.M. carried out all simulations. K.M., A.L.F., and K.L. designed the research, analyzed the data, and wrote the article.

ACKNOWLEDGMENTS

This work was, in part, supported by the National Institutes of Health (R01 HL120728, R01 HL151984) and the National Science Foundation CAREER (DMS-1848221).

DECLARATION OF INTERESTS

K.L. received research support from Novo Nordisk.

REFERENCES

1. Camerer, E., A. B. Kolstø, and H. Prydz. 1996. Cell biology of tissue factor, the principal initiator of blood coagulation. *Thromb. Res.* 81:1–41. <https://linkinghub.elsevier.com/retrieve/pii/004938489500209X>.
2. Furie, B., and B. C. Furie. 1992. Molecular and cellular biology of blood coagulation. *N. Engl. J. Med.* 326:800–806.
3. Maroney, S. A., P. E. Ellery, and A. E. Mast. 2010. Alternatively spliced isoforms of tissue factor pathway inhibitor. *Thromb. Res.* 125:S52–S56. <https://linkinghub.elsevier.com/retrieve/pii/S0049384810000915>.
4. Maroney, S. A., and A. E. Mast. 2015. New insights into the biology of tissue factor pathway inhibitor. *J. Thromb. Haemostasis.* 13:S200–S207. <https://doi.org/10.1111/jth.12897>.
5. Novotny, W. F., T. J. Girard, ..., G. J. Broze. 1988. Platelets secrete a coagulation inhibitor functionally and antigenically similar to the lipoprotein associated coagulation inhibitor. *Blood.* 72:2020–2025. <https://ashpublications.org/blood/article/72/6/2020/166184/Platelets-secrete-a-coagulation-inhibitor>.
6. Broze, G. J. 1995. Tissue factor pathway inhibitor and the revised theory of coagulation. *Annu. Rev. Med.* 46:103–112.
7. Sandset, P. M. 1996. Tissue factor pathway inhibitor (TFPI) – an update. *Haemostasis.* 26:154–165. <https://www.karger.com/Article/FullText/217293>.
8. Duga, S., R. Asselta, and M. L. Tenchini. 2004. Coagulation factor V. *Int. J. Biochem. Cell Biol.* 36:1393–1399. <https://linkinghub.elsevier.com/retrieve/pii/S1357272503002863>.
9. Segers, K., B. Dahlbäck, and G. A. F. Nicolaes. 2007. Coagulation factor V and thrombophilia: background and mechanisms. *Thromb. Haemostasis.* 98:530–542. <http://www.thieme-connect.de/DOI/DOI?10.1160/TH07-02-0150>.
10. Kuang, S.-Q., S. Hasham, ..., D. M. Milewicz. 2001. Characterization of a novel autosomal dominant bleeding disorder in a large kindred from east Texas. *Blood.* 97:1549–1554. <https://ashpublications.org/blood/article/97/6/1549/107333/Characterization-of-a-novel-autosomal-dominant>.
11. Vincent, L. M., S. Tran, ..., B. Dahlbäck. 2013. Coagulation factor VA2440G causes east Texas bleeding disorder via TFPI. *J. Clin. Invest.* 123:3777–3787. <http://www.jci.org/articles/view/69091>.
12. Broze, G. J., and T. J. Girard. 2013. Factor V, tissue factor pathway inhibitor, and east Texas bleeding disorder. *J. Clin. Invest.* 123:3710–3712. <http://www.jci.org/articles/view/71220>.

13. Wood, J. P., M. W. Bunce, ..., A. E. Mast. 2013. Tissue factor pathway inhibitor-alpha inhibits prothrombinase during the initiation of blood coagulation. *Proc. Natl. Acad. Sci. USA.* 110:17838–17843.
14. Schuitj, T. J., K. Bakhtiari, ..., C. van 't Veer. 2013. Factor Xa activation of factor V is of paramount importance in initiating the coagulation system: lessons from a tick salivary protein. *Circulation.* 128:254–266. <https://doi.org/10.1161/CIRCULATIONAHA.113.003191>.
15. Wood, J. P., P. E. R. Ellery, ..., A. E. Mast. 2014. Biology of tissue factor pathway inhibitor. *Blood.* 123:2934–2943. <https://ashpublications.org/blood/article/123/19/2934/32640/Biology-of-tissue-factor-pathway-inhibitor>.
16. Foster, W. B., M. E. Nesheim, and K. G. Mann. 1983. The factor Xa-catalyzed activation of factor V. *J. Biol. Chem.* 258:13970–13977.
17. Thorelli, E., R. J. Kaufman, and B. Dahlbäck. 1997. Cleavage requirements for activation of factor V by factor Xa. *Eur. J. Biochem.* 247:12–20.
18. Nicolaes, G. A. F., and B. Dahlbäck. 2002. Factor V and thrombotic disease: description of a janus-faced protein. *Arterioscler. Thromb. Vasc. Biol.* 22:530–538. <https://doi.org/10.1161/01.ATV.0000012665.51263.B7>.
19. Mann, K. G., and M. Kalafatis. 2003. Factor V: a combination of dr. Jekyll and mr. Hyde. *Blood.* 101:20–30. <https://ashpublications.org/blood/article/101/1/20/88938/Factor-V-a-combination-of-Dr-Jekyll-and-Mr-Hyde>.
20. Petrillo, T., F. Ayombil, ..., R. M. Camire. 2021. Regulation of factor V and factor V-short by TFPI: relationship between B-domain proteolysis and binding. *J. Biol. Chem.* 296:100234. <https://linkinghub.elsevier.com/retrieve/pii/S002192582000349X>.
21. Mast, A. E. 1996. Physiological Concentrations of Tissue Factor Pathway Inhibitor Do Not Inhibit Prothrombinase 1:1845–1850.
22. Wood, J. P., H. H. Petersen, ..., A. E. Mast. 2017. TFPIa interacts with FVa and FXa to inhibit prothrombinase during the initiation of coagulation. *Blood Adv.* 1:2692–2702.
23. Kuharsky, A. L., and A. L. Fogelson. 2001. Surface-mediated control of blood coagulation: the role of binding site densities and platelet deposition. *Biophys. J.* 80:1050–1074. <https://linkinghub.elsevier.com/retrieve/pii/S0006349501760857>.
24. Fogelson, A. L., and N. Tania. 2005. Coagulation under flow: the influence of flow-mediated transport on the initiation and inhibition of coagulation. *Pathophysiol. Haemostasis Thrombosis.* 34:91–108. <https://www.karger.com/Article/FullText/89930>.
25. Fogelson, A. L., Y. H. Hussain, and K. Leiderman. 2012. Blood clot formation under flow: the importance of factor XI depends strongly on platelet count. *Biophys. J.* 102:10–18. <https://linkinghub.elsevier.com/retrieve/pii/S0006349511013142>.
26. Leiderman, K., W. C. Chang, ..., A. L. Fogelson. 2016. Synergy between tissue factor and exogenous factor Xla in initiating coagulation. *Arterioscler. Thromb. Vasc. Biol.* 36:2334–2345. <https://doi.org/10.1161/ATVBAHA.116.308186>.
27. Link, K. G., M. T. Stobb, ..., K. Leiderman. 2018. A local and global sensitivity analysis of a mathematical model of coagulation and platelet deposition under flow. *PLoS One.* 13:e0200917. <https://dx.plos.org/10.1371/journal.pone.0200917>.
28. Link, K. G., M. T. Stobb, ..., K. B. Neeves. 2020. A mathematical model of coagulation under flow identifies factor V as a modifier of thrombin generation in hemophilia A. *J. Thromb. Haemostasis.* 18:306–317. <https://doi.org/10.1111/jth.14653>.
29. Hockin, M. F., K. C. Jones, ..., K. G. Mann. 2002. A model for the stoichiometric regulation of blood coagulation. *J. Biol. Chem.* 277:18322–18333.
30. Danforth, C. M., T. Orfeo, ..., K. E. Brummel-Ziedins. 2012. Defining the boundaries of normal thrombin generation: investigations into hemostasis. *PLoS One.* 7:e30385. <https://dx.plos.org/10.1371/journal.pone.0030385>.
31. Brummel-Ziedins, K. E., T. Orfeo, ..., K. G. Mann. 2009. Empirical and theoretical phenotypic discrimination. *J. Thromb. Haemostasis.* 7:181–186.
32. Miyazawa, K., A. L. Fogelson, and K. Leiderman. 2022. Inhibition of platelet-surface-bound proteins during coagulation under flow II: the role of antithrombin and heparin. *Biophys. J.*
33. Tracy, P. B., L. L. Eide, ..., K. G. Mann. 1982. Radioimmunoassay of factor V in human plasma and platelets. *Blood.* 60:59–63.
34. Steen, M., and B. Dahlbäck. 2002. Thrombin-mediated proteolysis of factor V resulting in gradual B-domain release and exposure of the factor Xa-binding site. *J. Biol. Chem.* 277:38424–38430. <https://linkinghub.elsevier.com/retrieve/pii/S0021925818363233>.
35. Monković, D. D., and P. B. Tracy. 1990. Functional characterization of human platelet-released factor V and its activation by factor Xa and thrombin. *J. Biol. Chem.* 265:17132–17140. <https://linkinghub.elsevier.com/retrieve/pii/S0021925817448794>.
36. Mann, K. G. 1987. The assembly of blood clotting complexes on membranes. *Trends Biochem. Sci.* 12:229–233. <https://www.sciencedirect.com/science/article/pii/0968000487901150>.
37. Krishnaswamy, S., K. C. Jones, and K. G. Mann. 1988. Prothrombinase complex assembly. Kinetic mechanism of enzyme assembly on phospholipid vesicles. *J. Biol. Chem.* 263:3823–3834. <https://linkinghub.elsevier.com/retrieve/pii/S0021925818689999>.
38. Jesty, J., T.-C. Wun, and A. Lorenz. 1994. Kinetics of the inhibition of factor Xa and the tissue factor-factor VIIa complex by the tissue factor pathway inhibitor in the presence and absence of heparin. *Biochemistry.* 33:12686–12694. <https://doi.org/10.1021/bi00208a020>.
39. Solymoss, S., M. M. Tucker, and P. B. Tracy. 1988. Kinetics of inactivation of membrane-bound factor Va by activated protein C. Protein S modulates factor Xa protection. *J. Biol. Chem.* 263:14884–14890. <https://linkinghub.elsevier.com/retrieve/pii/S0021925818681219>.
40. Thomassen, S., T. G. Mastenbroek, ..., J. W. M. Heemskerk. 2018. Suppressive role of tissue factor pathway inhibitor- α in platelet-dependent fibrin formation under flow is restricted to low procoagulant strength. *Thromb. Haemostasis.* 118:502–513.
41. Saltelli, A., P. Annoni, ..., S. Tarantola. 2010. Variance based sensitivity analysis of model output. Design and estimator for the total sensitivity index. *Comput. Phys. Commun.* 181:259–270. <https://linkinghub.elsevier.com/retrieve/pii/S0010465509003087>.
42. Saltelli, A., S. Tarantola, ..., M. Ratto. 2004. *Sensitivity Analysis in Practice: A Guide to Assessing Scientific Models.*
43. Baugh, R. J., G. J. Broze, and S. Krishnaswamy. 1998. Regulation of extrinsic pathway factor Xa formation by tissue factor pathway inhibitor. *J. Biol. Chem.* 273:4378–4386. <https://linkinghub.elsevier.com/retrieve/pii/S0021925818925603>.
44. Panteleev, M. A., V. I. Zarnitsina, and F. I. Ataullakhanov. 2002. Tissue factor pathway inhibitor: a possible mechanism of action. *Eur. J. Biochem.* 269:2016–2031.
45. Shibeko, A. M., E. S. Lobanova, ..., F. I. Ataullakhanov. 2010. Blood flow controls coagulation onset via the positive feedback of factor VII activation by factor Xa. *BMC Syst. Biol.* 4:5–12.
46. van 't Veer, C., and K. G. Mann. 1997. Regulation of tissue factor initiated thrombin generation by the stoichiometric inhibitors tissue factor pathway inhibitor, antithrombin-III, and heparin cofactor-II. *J. Biol. Chem.* 272:4367–4377.
47. Peterson, J. A., S. A. Maroney, and A. E. Mast. 2016. Targeting TFPI for hemophilia treatment. *Thromb. Res.* 141:S28–S30. <https://linkinghub.elsevier.com/retrieve/pii/S0049384816303590>.
48. Repke, D., C. H. Gemmell, ..., Y. Nemerson. 1990. Hemophilia as a defect of the tissue factor pathway of blood coagulation: effect of factors VIII and IX on factor X activation in a continuous-flow reactor. *Proc. Natl. Acad. Sci. USA.* 87:7623–7627.
49. Maroney, S. A., B. C. Cooley, ..., A. E. Mast. 2012. Absence of hematopoietic tissue factor pathway inhibitor mitigates bleeding in mice with hemophilia. *Proc. Natl. Acad. Sci. USA.* 109:3927–3931.
50. Erhardtzen, E., M. Ezban, ..., O. Nordfang. 1995. Blocking of tissue factor pathway inhibitor (TFPI) shortens the bleeding time in rabbits

with antibody induced hemophilia A. *Blood Coagul. Fibrinolysis*. 6:388–394.

51. Broze, G. J., Jr., G. W. Lange, ..., L. MacPhail. 1994. Heterogeneity of plasma tissue factor pathway inhibitor. *Blood Coagul. Fibrinolysis*. 5:551–559. <https://europepmc.org/article/med/7841311>.

52. Augustsson, C., I. Hilden, and L. C. Petersen. 2014. Inhibitory effects of LDL-associated tissue factor pathway inhibitor. *Thromb. Res.* 134:132–137.

53. Gierula, M., and J. Ahnström. 2020. Anticoagulant protein S—new insights on interactions and functions. *J. Thromb. Haemostasis*. 18:2801–2811.

54. Dahlbäck, B., L. J. Guo, ..., S. Tran. 2018. Factor V-short and protein S as synergistic tissue factor pathway inhibitor (TFPI α) cofactors. *Res. Pract. Thromb. Haemost.* 2:114–124.

55. Dahlbäck, B., and S. Tran. 2022. The preAR2 region (1458–1492) in factor V-Short is crucial for the synergistic TFPI α -cofactor activity with protein S and the assembly of a trimolecular factor Xa-inhibitory complex comprising FV-Short, protein S, and TFPI α . *J. Thromb. Haemostasis*. 20:58–68.

56. Dahlbäck, B., and S. Tran. 2022. A hydrophobic patch (PLVIVG; 1481–1486) in the B-domain of factor V-short is crucial for its synergistic TFPI α -cofactor activity with protein S and for the formation of the FXa-inhibitory complex comprising FV-short, TFPI α , and protein S. *J. Thromb. Haemostasis*. 20:1146–1157.

57. Maroney, S. A., and A. E. Mast. 2008. Expression of tissue factor pathway inhibitor by endothelial cells and platelets. *Transfus. Apher. Sci.* 38:9–14. <https://linkinghub.elsevier.com/retrieve/pii/S1473050207001759>.